

Structure-based drug design of chromone antagonists of the adenosine A_{2A} receptor†

Cite this: DOI: 10.1039/c3md00338h

Stephen P. Andrews,†* Jonathan S. Mason, Edward Hurrell and Miles Congreve

Received 4th November 2013
Accepted 30th December 2013

DOI: 10.1039/c3md00338h

www.rsc.org/medchemcomm

The structure-guided optimisation of a hit series of chromone derivatives, previously identified using virtual screening of homology models of the adenosine A_{2A} receptor, has led to the discovery of potent, selective and ligand efficient antagonists. Lipophilic hotspots and calculated water networks were modelled within the receptor binding site to facilitate rational ligand design.

High resolution crystal structures have been published for twenty G protein-coupled receptors (GPCRs), including 17 members of the rhodopsin family, a frizzled receptor and two members of the secretin family.^{1–4} These advances in structural biology have given enormous insight into the binding sites of this superfamily of receptors, facilitating structure-based drug design and providing templates for the construction of high confidence homology models.^{5–7}

The adenosine A_{2A} receptor is a member of the rhodopsin family of GPCRs (class A). Many ligands are known for this receptor, including a number of antagonists which have been investigated clinically for the treatment of central nervous system disorders, particularly Parkinson's disease.⁸ For example, preladenant reached phase 3 clinical trials but was discontinued owing to lack of efficacy *versus* placebo and, in 2013, istradefylline was launched in Japan for the treatment of Parkinson's disease. Currently, there are no other marketed A_{2A} receptor antagonists and the exploration of further chemotypes is warranted.

Compound **1** was previously reported as a 2.0 μM hit following the virtual screening of homology models of the A_{2A} receptor which were built from the crystal structure of the β₁ adrenergic receptor.⁹ Herein, we describe the efficient optimisation of a series of chromone ligands with structure-based approaches driven by molecular modelling and biophysical techniques.

Compound **1** was identified prior to solving the X-ray crystal structure of the A_{2A} receptor; however, there are now multiple 3D structures available for this receptor, which has been solved in both its active and inactive forms,¹⁰ facilitated by either a fusion protein¹¹ or thermostabilisation technology.¹²

Initial analysis of **1** with the A_{2A} receptor homology models resulted in two putative binding modes (A and B; Fig. 1), from Glide¹³ docking studies. In order to improve the activity of **1** by rational design it was first necessary to validate binding mode A which, after further modelling and careful analysis, appeared to be the most plausible. To this end, small sets of analogues were designed iteratively and tested in a competitive radioligand binding assay¹⁴ with hA_{2A} receptor and [³H]-ZM241385.

Initially, the negatively charged carboxylate functionality was removed from **1** as it had been modelled to sit unfavourably in a lipophilic region lined by Leu167^{ECL2}, Ile66^{2,64} and Met270^{7,35} (superscript numbers refer to Ballesteros–Weinstein¹⁵ numbering). As predicted, replacement with a positively charged group such as an aliphatic amine (**2**) did not invoke an increase in affinity, whereas conversion to a neutral group such as an ester (**3**) gave rise to a 20-fold improvement in affinity (Table 1).

Modifications with simple alkyl groups led to improvements in ligand efficiency¹⁶ (**4**; LE = 0.42), and larger chains were also well-tolerated (**5**; pK_i = 7.6). A simple acetate group at position R¹ was found to maintain a good level of affinity (**6**) and the

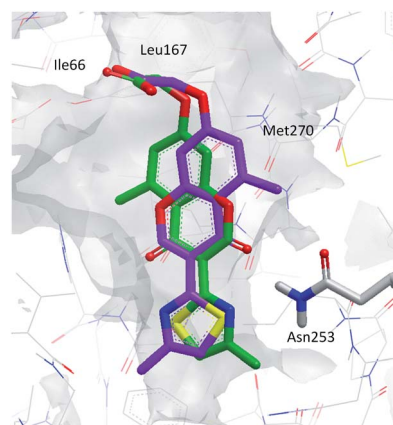


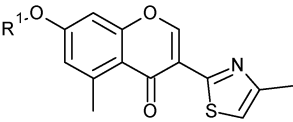
Fig. 1 Putative binding modes of compound **1**. In mode A (green carbon) the thiazole N hydrogen bonds to Asn253 and in mode B (purple carbon) the chromone carbonyl group hydrogen bonds to Asn253.

Heptares Therapeutics Ltd., Biopark, Broadwater Road, Welwyn Garden City, AL7 3AX, UK. E-mail: steve.andrews@heptares.com

† Electronic supplementary information (ESI) available. See DOI: 10.1039/c3md00338h

‡ ©Heptares Therapeutics 2013. The HEPTARES name is a trade mark of Heptares Therapeutics Ltd.

Table 1 Initial hit exploration

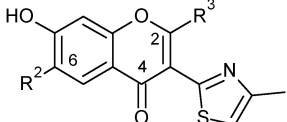
			
	R ¹	pK _i	LE
1	–CH ₂ CO ₂ H	5.7	0.34
2	–(CH ₂) ₂ NMe ₂	5.8	0.33
3	–CH ₂ CO ₂ Et	7.0	0.38
4	–methylcyclopropyl	7.1	0.42
5	–(CH ₂) ₃ C≡CH	7.6	0.43
6	–C(=O)Me	7.5	0.46
7	–H	6.5	0.47

unsubstituted hydroxyl derivative (7) showed the highest LE (0.47). This phenol group was kept constant in the following round of design where the effects of substituents at other positions on the chromone scaffold were rationally explored.

During a druggability analysis,⁶ a lipophilic hotspot was identified with a GRID aromatic CH (C1=) probe,¹⁷ in a pocket lined by Ile66^{2,64} and Tyr271^{7,36} (Fig. 2). This led to the design of compounds with lipophilic groups at the vector defined by R² (C-6 of the chromone core), with the minimum chain length of two atoms required to reach the hotspot (Table 2). When compared to the R²-unsubstituted derivative (8), compounds 9, 10 and 11 all showed very good affinities for the receptor.

The size of the lipophilic hotspot indicated that a propyl group would most efficiently fill this pocket and this was indeed found to be the case, with 10 showing the highest LE. A later analysis using WaterFLAP and WaterMap in conjunction with A_{2A} receptor crystal structures showed that moderately high energy or 'unhappy' waters⁶ are in this region and are displaced by 10 (see ESI†). The larger *n*-pentyl derivative (11) explores

Table 2 Investigation of substituents at vectors R² and R³

				
	R ²	R ³	pK _i	LE
8	H	H	5.7	0.44
9	Et	H	7.1	0.49
10	<i>n</i> -Pr	H	7.6	0.50
11	<i>n</i> -pentyl	H	7.7	0.46
12	H	Me	5.1	0.37

areas outside of the hotspot and shows only a small increase in potency when compared to 10. Compounds 9 and 10 were therefore progressed in preference to 11 as they showed the best balance of LE and lipophilic ligand efficiency¹⁸ (LLE = 3.6, 3.7 and 2.8, respectively).

The proposed binding mode (A) was further confirmed by testing compound 12 with a methyl substituent at position R³. Compound 12 was predicted to impose a steric clash on Asn253^{6,55} in binding mode A (Fig. 2; the carbon at position C-2 of the chromone is almost at the GRID C3 surface), and was found to be four times less active than 8. By contrast, in binding mode B, the methyl group of 12 would face a large pocket and a minimal change of activity would be expected (see Fig. 1).

Selected analogues from this series were screened for stability in rat liver microsomes (RLM) and selectivity *vs.* the adenosine A₁ receptor. They were found to have half-lives in RLM of 14–18 minutes (see ESI†) and, in several cases, much higher affinity was observed for the A_{2A} receptor than the A₁ receptor. For example, compound 6 was 13-fold selective for the A_{2A} receptor and compounds 4, 9 and 11 were all >100-fold selective for the A_{2A} receptor (see ESI†). In order to understand and rationalise these observations, homology models of the A₁ receptor were constructed from crystal structures of the A_{2A} receptor.

Compound 4 contains a bulky and lipophilic methylcyclopropyl group at vector R¹ which, in the A_{2A} receptor binding site, sits in a lipophilic sub-pocket with a relatively large cavity. This pocket was found to be smaller and more polar in the corresponding A₁ site, thus disfavouring the binding of 4 (Fig. 3).

Compound 11 contains a lipophilic group at the vector R², and this group also sits in a sub-pocket which is smaller and more polar in the A₁ binding site. In A_{2A}, the polar hydroxyl of Ser67^{2,65} was found to point away from the sub-pocket (Fig. 2), whereas in A₁, the corresponding residue (Asn70^{2,65}) was modelled with its polar side chain facing into the binding site, H-bonding to the backbone of Ala66^{2,61}, or to Gln9^{1,32} and Tyr271^{7,36}.

To further corroborate these findings, compound 8 was found to have a two-fold higher affinity for the adenosine A₁ receptor, as it does not have substituents at either vector R¹ or R² to access these 'selectivity pockets'.

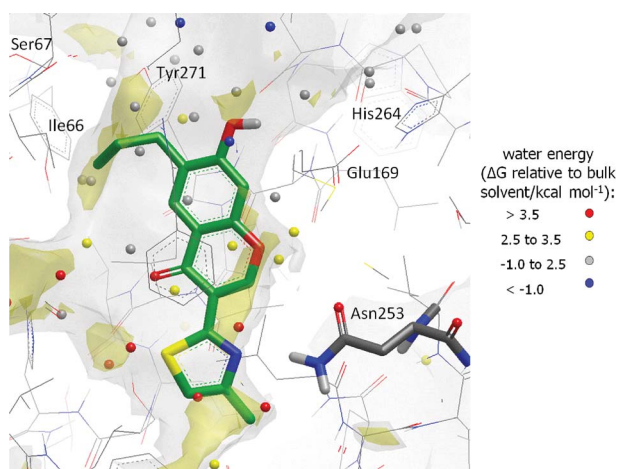


Fig. 2 Compound 10 in binding mode A; GRID C3 surface (1.0 kcal mol^{–1}; grey) and C1= lipophilic hotspots (–2.8 kcal mol^{–1}; yellow) for A_{2A} receptor; and WaterMap waters calculated for the pseudo-apo protein from the ligand complex PDB:3UZC (coloured spheres).

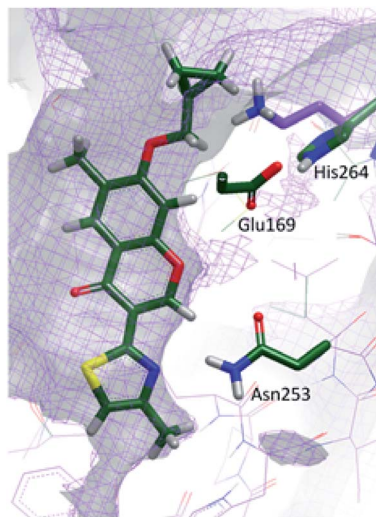


Fig. 3 Compound **4** modelled in the 1.8 Å resolution A_{2A} receptor crystal structure (PDB: 4E1Y), with its GRID C3 surface shown in solid grey. In this model, His264^{ECL3} H-bonds to Glu169^{ECL2} which leaves its aromatic ring facing the binding site and creates a lipophilic cavity. In the corresponding A_1 receptor model (also based on PDB: 4E1Y; GRID C3 surface shown in lilac mesh), the longer Lys265^{ECL3} (shown in lilac stick) moves into the cavity to interact with Glu172^{ECL2} (Glu169^{ECL2} in A_{2A}), thus changing the size and polarity of the pocket. The cyclopropyl group of **4** is seen to pierce the A_1 pocket (see ESI†).

Compound **13** was selected as a representative of the series and tested for affinity at all of the adenosine receptor sub-types: A_{2A} , A_1 , A_{2B} and A_3 . It was found to have >100-fold higher affinity for the A_{2A} receptor than the A_1 receptor, and no measurable binding affinity for the A_{2B} or A_3 receptors (Fig. 4).

The combination of the SAR observed in Table 1 and 2 led to compound **14** which was found to have a good affinity for the A_{2A} receptor and maintained a high LE (Fig. 5; LE = 0.48, pK_i = 8.5). Subsequent Biophysical Mapping™ (BPM – a technique which combines site-directed mutagenesis with surface plasmon resonance screening in order to determine the individual contributions of binding site residues to the binding of ligands)¹⁹ of **14** suggested that the propyl group of this ligand

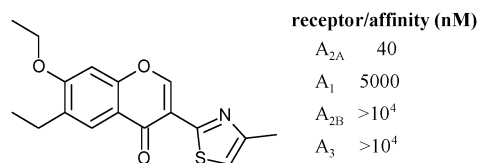


Fig. 4 Compound **13**.

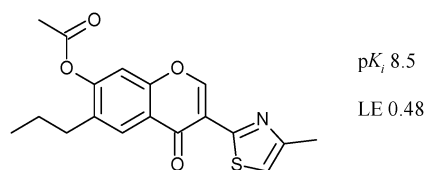


Fig. 5 Compound **14**.

interacted with Ile66^{ECL2} and Tyr271^{7,36}, which further supports binding mode A, in which the chromone C-6 substituent is projected towards this lipophilic sub-pocket of the binding site.⁹

The final area of the molecules to be investigated was the 4-methylthiazole group. The N atom of this heterocycle provides the core H-bond found for A_{2A} receptor ligands to Asn253^{6,55}. Furthermore, the methyl group at the 4 position of this heterocycle makes a crucial contribution to the binding affinity of this series of molecules, with a severe (33-fold) loss of activity upon its removal (**16** → **17**; Table 3). This is a clear example of a 'magic methyl' effect, and is of similar magnitude to a recent example published with opioid receptor antagonists,²⁰ but here there is a clear structural understanding of its origin. The methyl group displaces an 'unhappy' water (red sphere in Fig. 2), identified from a WaterMap calculation of the water network and energetics for the pseudo-apo X-ray structure from PDB: 3UZC.^{6,14,21,22} This water is in a lipophilic hotspot cavity in the binding site, giving a strong beneficial effect; furthermore, without the thiazole methyl group, this water would be trapped in an even more unfavourable position (owing to the remaining apolar CH of the ligand), that would bind less deeply or create a 'dewetted' vacuum region.²³ This phenomenon was not observed with ZM241385 which contains a furan ring that sits more deeply than the thiazole of **14** and is unable to accommodate a methyl substituent (Fig. 6).

The power of water network energetic analyses to rationalise SAR and drive ligand design is further illustrated when changing the position of the sulphur atom within the thiazole ring. A ten-fold reduction in activity is found between compounds **14** and **15**, yet no changes in favourable interactions or steric clashes are observed with the receptor. Both ligands are still able to hydrogen bond to Asn253^{6,55} via their N atoms. Scoring of the two isomers using the docking program Glide in both SP and XP modes showed insignificant differences (approx. 0.1 kcal better or worse, respectively) and no differences were observed in a rescoring with Hyde²⁴ that

Table 3 Investigation of the methylthiazole substituent

	R ⁴	R ⁵	pK_i	LE
15	Me		7.5	0.43
16	H		7.3	0.43
17	H		5.8	0.36

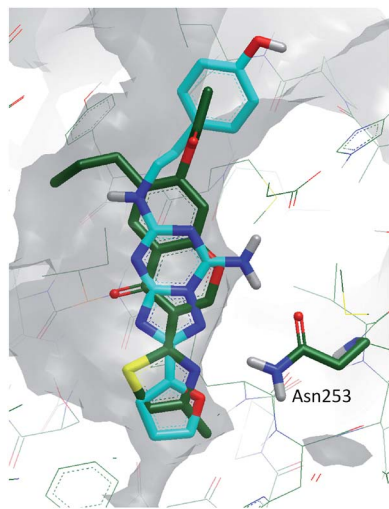


Fig. 6 Compound **14** (green stick), modelled in the 1.8 Å resolution structure of the A_{2A} receptor (PDB: 4EIY). ZM241385 (cyan stick) is shown to bind very deeply with the furan C5 atom touching the surface of the binding site (GRID C3 surface shown in solid grey).

explicitly considers hydrophobic interactions *via* atom logP contributions.

The significant difference in potency observed with this small change of an indirectly-interacting ligand atom can be rationalized by analysing the computed energies of the waters in the bottom of the pocket (affected in **15** by the S atom; Fig. 7) and the left of the pocket (affected in **14** by the S atom). Using the sum of the energies of the GRID probes for water and C1= in WaterFLAP, the two waters at the bottom of the pocket were found to increase in energy by 9 kcal (**14** → **15**), whereas the five waters to the left were only 4.5 kcal lower. The significant increase in the total energy of the waters affected by **14** → **15** could thus rationalise the potency drop.

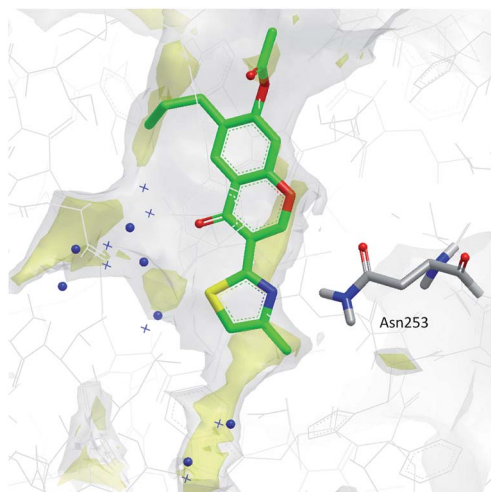


Fig. 7 Waters in the proximity of the thiazole ring from the computed water networks for **14** (blue spheres; ligand shown) and **15** (blue crosses; ligand not shown) from a WaterFLAP analysis, used to compare water network perturbation.

In summary, the structure-guided optimization of a chromone hit series has led to the discovery of potent antagonists of the A_{2A} receptor with high LE and selectivity. Important aspects of the series' SAR can be explained by the effect of displacing waters from lipophilic hotspots ('unhappy' waters) or by perturbing the calculated water network within the binding site. This study is an example of how high quality GPCR binding mode information is starting to significantly impact on the discovery of new agents for this important class of receptors. In particular, the ability to consider the position and energy of lipophilic hotspots and of calculated water molecules offers great promise for rational drug design.

Notes and references

- 1 N. Bertheleme, P. S. Chae, S. Singh, D. Mossakowska, M. M. Hann, K. J. Smith, J. A. Hubbard, S. J. Dowell and B. Byrne, *Biochim. Biophys. Acta, Gen. Subj.*, 2013, **1828**, 2583.
- 2 C. Wang, H. Wu, V. Katritch, G. W. Han, X. P. Huang, W. Liu, F. Y. Siu, B. L. Roth, V. Cherezov and R. C. Stevens, *Nature*, 2013, **497**, 338.
- 3 K. Hollenstein, J. Kean, A. Bortolato, R. K. Cheng, A. S. Dore, A. Jazayeri, R. M. Cooke, M. Weir and F. H. Marshall, *Nature*, 2013, **499**, 438.
- 4 F. Y. Siu, M. He, G. C. de, G. W. Han, D. Yang, Z. Zhang, C. Zhou, Q. Xu, D. Wacker, J. S. Joseph, W. Liu, J. Lau, V. Cherezov, V. Katritch, M. W. Wang and R. C. Stevens, *Nature*, 2013, **499**, 444.
- 5 B. Kobilka, *Angew. Chem., Int. Ed.*, 2013, **52**, 6380.
- 6 J. S. Mason, A. Bortolato, M. Congreve and F. H. Marshall, *Trends Pharmacol. Sci.*, 2012, **33**, 249.
- 7 M. Congreve, C. J. Langmead, J. S. Mason and F. H. Marshall, *J. Med. Chem.*, 2011, **54**, 4283.
- 8 J. F. Chen, H. K. Eltzhig and B. B. Fredholm, *Nat. Rev. Drug Discovery*, 2013, **12**, 265.
- 9 C. J. Langmead, S. P. Andrews, M. Congreve, J. C. Errey, E. Hurrell, F. H. Marshall, J. S. Mason, C. M. Richardson, N. Robertson, A. Zhukov and M. Weir, *J. Med. Chem.*, 2012, **55**, 1904.
- 10 S. P. Andrews and B. Tehan, *Med. Chem. Commun.*, 2013, **4**, 52.
- 11 E. Chun, A. A. Thompson, W. Liu, C. B. Roth, M. T. Griffith, V. Katritch, J. Kunken, F. Xu, V. Cherezov, M. A. Hanson and R. C. Stevens, *Structure*, 2012, **20**, 967.
- 12 N. Robertson, A. Jazayeri, J. Errey, A. Baig, E. Hurrell, A. Zhukov, C. J. Langmead, M. Weir and F. H. Marshall, *Neuropharmacology*, 2011, **60**, 36.
- 13 T. A. Halgren, R. B. Murphy, R. A. Friesner, H. S. Beard, L. L. Frye, W. T. Pollard and J. L. Banks, *J. Med. Chem.*, 2004, **47**, 1750.
- 14 M. Congreve, S. P. Andrews, A. S. Dore, K. Hollenstein, E. Hurrell, C. J. Langmead, J. S. Mason, I. W. Ng, B. Tehan, A. Zhukov, M. Weir and F. H. Marshall, *J. Med. Chem.*, 2012, **55**, 1898.
- 15 J. A. Ballesteros, H. Weinstein, and C. S. Stuart, in *Methods in Neurosciences*, Academic Press, New York, 1995, vol. 25, pp. 366–428.

- 16 A. L. Hopkins, C. R. Groom and A. Alex, *Drug Discovery Today*, 2004, **9**, 430.
- 17 P. J. Goodford, *J. Med. Chem.*, 1985, **28**, 849.
- 18 P. D. Leeson and B. Springthorpe, *Nat. Rev. Drug Discovery*, 2007, **6**, 881.
- 19 A. Zhukov, S. P. Andrews, J. C. Errey, N. Robertson, B. Tehan, J. S. Mason, F. H. Marshall, M. Weir and M. Congreve, *J. Med. Chem.*, 2011, **54**, 4312.
- 20 G. Lunn, B. J. Banks, R. Crook, N. Feeder, A. Pettman and Y. Sabnis, *Bioorg. Med. Chem. Lett.*, 2011, **21**, 4608.
- 21 A. Bortolato, B. G. Tehan, M. S. Bodnarchuk, J. W. Essex and J. S. Mason, *J. Chem. Inf. Model.*, 2013, **53**, 1700.
- 22 C. Higgs, T. Beuming and W. Sherman, *ACS Med. Chem. Lett.*, 2010, **1**, 160.
- 23 J. S. Mason, A. Bortolato, D. R. Weiss, F. Deflorian, B. Tehan and F. H. Marshall, *In Silico Pharmacology*, 2013, **1**, 1.
- 24 N. Schneider, S. Hindle, G. Lange, R. Klein, J. Albrecht, H. Briem, K. Beyer, H. Claussen, M. Gastreich, C. Lemmen and M. Rarey, *J. Comput.-Aided Mol. Des.*, 2012, **26**, 701.